Journal of Physics:
Conference Series



**PAPER** • **OPEN ACCESS**

# Exergo-economic and exergo-environmental analysis of a binary geothermal power plant with solar boosting

To cite this article: E. Giusti *et al* 2022 *J. Phys.: Conf. Ser.* **2385** 012124

# Exergo-economic and exergo-environmental analysis of a binary geothermal power plant with solar boosting

**E. Giusti, L. Ciappi, P. Ungar, C. Zuffi, D. Fiaschi, G. Manfrida, L. Talluri**

University of Florence, Florence, Italy

Corresponding author's e-mail address: pietro.ungar@unifi.it

**Abstract**. The exploitation of renewable energies is a solution to the energy, economic and environmental issues related to the massive use of fossil resources. Thus, investing in renewable technologies is essential to achieve the carbon-neutral scenario within 2050. In this framework, geothermal energy may have a key role. In particular, power plants with a closed binary cycle are suitable for harnessing geothermal resources with low and medium enthalpy levels. They are prone to be integrated with other renewable devices to increase the global power output.

Geothermal fluid can be drawn constantly from underground throughout the day and seasons. Conversely, the availability and intensity of solar energy depend on weather conditions and the time of year. In Italy, geothermal energy is currently harvested for continuous electricity generation, while solar energy is mainly used for photovoltaic generation. For small-to-medium size plants, rated between 5 and 20 MWe, the geothermal and thermodynamic solar hybridization may lead to relevant benefits for the economic competitiveness regarding separate photovoltaic or thermodynamic solar systems.

This article aims to investigate the economic and environmental aspects of geothermal power plants with a closed binary cycle coupled with a topper cycle fed by linear parabolic solar collectors. The system operation in both design and off-design conditions was analysed, and exergo-economic and exergo-environmental simulations were conducted. The application site was selected near Torre Alfina (Italy). It has a water-dominant reservoir with a pressure of 44 bar, a temperature of 140 °C, and content of non-condensable gases (NCGs) approximately equal to 2% by weight. At the design point, the net power is 8.4 MW and the first and second principle efficiencies are 9.31% and 18.45%, respectively. The exergo-economic and exergo-environmental analyses indicate that the components with the highest economic and environmental impact are the condenser, the field of solar collectors, the evaporator, and the low-pressure turbine. The levelized cost of electricity (LCOE) is equal to 14.19 c€/kWh.

## 1. Introduction

Geothermal energy can significantly contribute to solve the issue of the depletion of fossil fuels and the economic and environmental problems consequent to their massive use. However, geothermal power plants are not free of environmental impacts, which may be evaluated through a life cycle assessment (LCA).

Above all, the release of non-condensable gasses (NCGs) from the geothermal brine into the atmosphere is one of the most impacting of these issues. In the Italian geothermal reservoirs, the NCGs are mainly composed of $CO_2$ and represent up to 10% in mass of the extracted brine. Moreover, they contain significant contaminants such as $CH_4$, $H_2S$, $NH_3$, Hg, and heavy metals [1, 2]. Typical geothermal power plants such as dry steam and single and double flash plants using high enthalpy reservoirs apply abatement approaches to reduce these contaminants. For instance, in Italy, the AMIS® (Hydrogen Sulfide and Mercury Abatement System) technology [3] is utilized for chemical scrubbing and adsorption and effectively removes $H_2S$, $NH_3$, and Hg. However, this approach does not solve the problem of greenhouse gas emissions, estimated at around 122 mg/kWh [4, 5]. For this reason, other geothermal solutions were studied to reduce the environmental impact. One of the most

 2385 (2022) 012124 doi:10.1088/1742-6596/2385/1/012124 

promising ones is the total reinjection of working fluids, which avoids emissions and allows the preservation of the reservoir. Hybridization with other renewable resources provides for increased energy harvesting. In particular, the present research focuses on hybridizing a geothermal system with parabolic trough collectors (PTCs). This solution allows combining the good trait of both resources through the base load of the geothermal device and the peak load of the solar device for a limited time of hours, reducing thus the required soil occupation of the collectors.

## 2. Site and power plant of Torre Alfina

The case study selected for the application of the proposed solution is situated near Torre Alfina. The geothermal site comprises a water-dominated reservoir with a pressure of about 44 bar and a temperature of 140 °C [13, 14]. It has a relatively moderate amount of NCGs consisting of about the 2% of $CO_2$ and 0.2% of $H_2S$ [15, 16, 17].

Five production wells and four reinjection wells generate around 5 MWe, which is the size of a pilot power plant for the Italian regulations [18].

The space available at the site makes it possible to combine the geothermal power plant with a topper cycle fed by linear parabolic solar collectors. Thus, the ORC system with two pressure levels shown in Figure 1 is obtained, and the power output is enhanced.

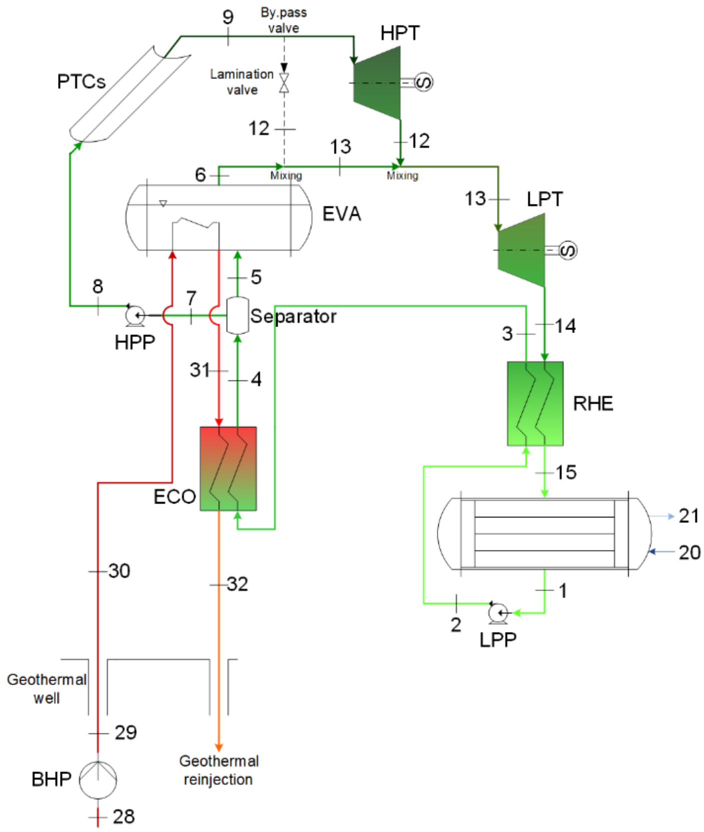


*Figure 1. General layout of the new hybrid power plant with brine, ORC, and solar circuits*

The plant is designed to separate part of the fluid from the economizer when direct solar radiation is present for delivering it to the solar field for vaporization. At first, the HP steam generated by the PTCs evolves in the high-pressure turbine; then, it is mixed with the steam from the geothermal evaporator, and the mixture develops in the LP turbine. The flow rate in the PTCs decreases with the solar radiation until the minimum value allowed in the HP turbine of around 40% of the design flow rate is reached. By this time, a by-pass circuit is activated, and the fluid expands through a lamination valve. Finally, when no direct solar irradiation is present, the separator is closed, and the power plant operates as a conventional geothermal system. Table 1 resumes the main parameters of the plant, where $T$ is the temperature $p$ is the pressure $w$ is the weight, $\dot{m}$ is the mass flow rate, $\eta$ is the efficiency, $\Delta$ is the difference, *LP/HP* is the ratio between the low and high values of the pressure, and the subscripts $T$, $P$, and $pp$ refert to the turbine, the pump, and the pinch point, respectively.

Table 1. Main parameters of the new hybrid Torre Alfina power plant

| | | | |
|---|---|---|---|
| $T_{30}$ [°C] | 140 | $\dot{m}_{13}$ [kg/s] | 234.8 |
| $p_{30}$ [bar] | 44 | $p_9$ [bar] | 30 |
| $CO_2$ [$w$%] | 2 | $T_9$ [°C] | 150 |
| $\dot{m}_{30}$ [kg/s] | 234.9 | $\dot{m}_9$ [kg/s] | 53.64 |
| Working fluid | Isobutane | $\eta_{LPT}$, $\eta_{LPP}$, $\eta_{HPT}$, $\eta_{HPP}$ | 0.87, 0.8, 0.87, 0.8 |
| $T_6$ [°C] | 85 | $\Delta T_{pp}$ | 10 |
| $p_{13}$ [bar] | 14.82 | | |

## 3. Energy, exergy, exergo-economic, and exergo-environmental modeling

Thermodynamic and exergy analyses were carried out by applying the mass, energy, and exergy balances proposed in [20]. Following the approach of [19] for the properties of the geothermal fluid, the specific libraries available in Unisim® or TREND 3.0 were used. The internal libraries of the Engineering Equation Solver (EES) software were utilized to calculate the thermodynamic properties of the working fluid [21]. The reference state for the exergy analysis was set at 15 °C and 101.325 kPa.

The exergo-economic analysis (EEA) combines the exergy analysis with the cost analysis of the power plant equipment. The "fuel" and a "product" were defined for each plant component, following the SPECO (SPecific Exergy COsting) approach [22]. Most of the equipment costs (Table 2) needed for the EEA were calculated using validated cost correlations [23, 24] reported in equations from 1 to 3 and updated by applying the latest CEPCI (Chemical Engineering Plant Cost Index).

Table 2. Correlations applied for defining the Equipment costs

| **Component** | **Cost-correlation [€]** | **Component** | **Cost-correlation [€]** |
|---|---|---|---|
| Borehole (BH) pump | $1000 \cdot W_{BHP}$ | Condenser (COND) | *Eq. (1)* |
| LPP | *Eq. (1)* | HPP | *Eq. (1)* |
| Regenerative Heat Exchanger (RHE) | *Eq. (1)* | PTCs | 250 \$/m$^2 \cdot A_{PTCs}$ |
| Economiser (ECO) | *Eq. (1)* | HPT | *Eq. (1)* |
| Separator | *Eq. (1)* | Mixing 2 | 0 |
| Evaporator (EVA) | *Eq. (1)* | Lamination valve | 1000 |
| LPT | *Eq. (1)* | Mixing 1 | 0 |

$$C_{BM} = C_p^0 * F_{BM} \quad (1)$$

$$\log_{10} C_p^0 = K_1 + K_2 \log_{10}(X) + K_3(\log_{10}(X))^2 \quad (2)$$

$$F_{BM} = (B_1 + B_2 F_p F_M) \quad (3)$$

where $W_{BHP}$ is the power of the borehole pump, $A_{PTCs}$ is the area of the surface of the filed of solar collectors, $C_{BM}$ is the cost of the bare module including its direct and indirect costs, $C_p{}^0$ is the base cost of the component, $F_{BM}$ is the bare module factor considering the cost correction based on the pressure and material of the component, $X$ is the functional unit of the component and $K_1$, $K_2$, $K_3$, $B_1$, $B_2$, $F_P$, $F_M$ are correction coefficients defined by [24].

In the case of a binary geothermal power plant, the cost of the production and reinjection wells is relevant, and it is determined through consolidated correlations [25]. The cost of geothermal and solar energy is considered null, following the traditional practice of renewable energy applications. The cost of the PTCs was derived from the literature [27]. The cost of the condenser loss is calculated and re-assigned to all the streams proportionally to the flow of the "fuel" exergy [20].

The exergo-economic analysis allows the calculation of the energy transformation cost. It provides insight into the possibilities of power plant improvement by identifying the components responsible for the highest costs of exergy destruction and capital.

The last step of this study was assessing the environmental performance of the power plant. For this purpose, an exergo-environmental analysis (EEvA) was carried out. The EEvA combines the exergy analysis with the LCA. The values of environmental impacts were calculated by scaling the values obtained for the geothermal bottom plant from [19] and the solar field from [28]. Each was scaled regarding its functional unit and under the same conditions as the environment considered in this study. In particular, the construction phase, specifically the drilling of the wells, is relevant for the life cycle impact assessment (LCIA) of a geothermal power plant [29] and for the hybrid power plant. Regarding the wells and the machinery equipment, data about the specific material consumption used LCA process were collected in [19] from the environmental assessments provided by [30].

The main results of the exergo-economic and exergo-environmental analyses are the coefficients described in Table 3 and calculated for each component of the plant, where $\dot{Ex}$ is the Exergy rate, $\dot{Z}$ is the instantaneous capital cost, $\dot{C}_D$ is the exergy destruction cost rate, $c_F$ is the cost of the fuel, $c_P$ is the cost of the product, and $b$ is the specific environmental impact rate.

Table 3. Main coefficients used in the exergo-economic and exergo-environmental analyses

| **Exergo-economic analysis** | **Exergo-environmental analysis** |
|---|---|
| Exergy stream cost rate [€/s] $\dot{C}_j = c_j \cdot \dot{Ex}_j$ | Exergo-environmental stream impact rate [Pts/s] $\dot{B}_j = b_j \cdot \dot{Ex}_j$ |
| Component cost balance $\sum \dot{C}_{j,k,in} + \dot{Z}_k = \sum \dot{C}_{j,k,out}$ | Component environmental impact balance $\sum \dot{B}_{j,k,in} + \dot{Y}_k = \sum \dot{B}_{j,k,out}$ |
| Component-related cost (Table 2) | Component-related environmental impact rate $\dot{Y}_k = \dot{Y}_{CO} + \dot{Y}_{OM} + \dot{Y}_{DI}$ |
| Component exergo-economic factor $f_k = \frac{\dot{Z}_k}{\dot{Z}_k + \dot{C}_{D,k}}$ | Component exergo-environmental factor $f_{d,k} = \frac{\dot{Y}_k}{\dot{Y}_k + \dot{B}_{D,k}}$ |
| Component relative cost difference $r_k = \frac{c_{P,k} - c_{F,k}}{c_{F,k}}$ | Component relative difference of specific environmental impacts $r_{b,k} = \frac{b_{P,k} - b_{F,k}}{b_{F,k}}$ |

In this study, the EEA and the EEvA were carried out using the 3ETool software developed in Python [31].

The data on the temperature and pressure and the solar irradiance of the Torre Alfina site throughout the year were obtained from PVGIS [32]. In this article, the typical monthly day is analyzed. The orientation of the solar field in both N-S and E-O directions was investigated to verify that the N-S direction provides the highest energy collection as suggested in [33, 34]. Since, PVGIS provides only the monthly typical day data of irradiance either for a fixed plane oriented and inclined by fixed angles or for two-axis solar tracking, a spreadsheet was obtained by importing the PVGIS data relating to the DNI on a fixed horizontal plane and oriented in both N-S and E-O directions. Then, the data of DNI for a single-axis solar tracking were calculated using formulas available in the literature [35]. The results confirmed that for Torre Alfina latitude, the greatest amount of annual direct solar radiation occurs for solar tracking around the N-S axis.

Since the environmental conditions provided by PVGIS differ from those used in the previous article [19], the performance of the system in [19] was recalculated considering the same environmental conditions adopted in this new study for comparing the results.

## 4. Thermodynamic analysis at the design point and heat exchanger sizing

The system was designed for the condition expected in June at 11 a.m. when the maximum annual radiation is present. The maximum temperature reached by the collectors is evaluated by a procedure minimizing their levels of exergy inefficiency [36]. At the design point, the temperature is 150 °C. In Figure 2, the temperature is presented to the changes of the specific entropy *s* for both the single geothermal system and the new hybrid geothermal and solar systems.

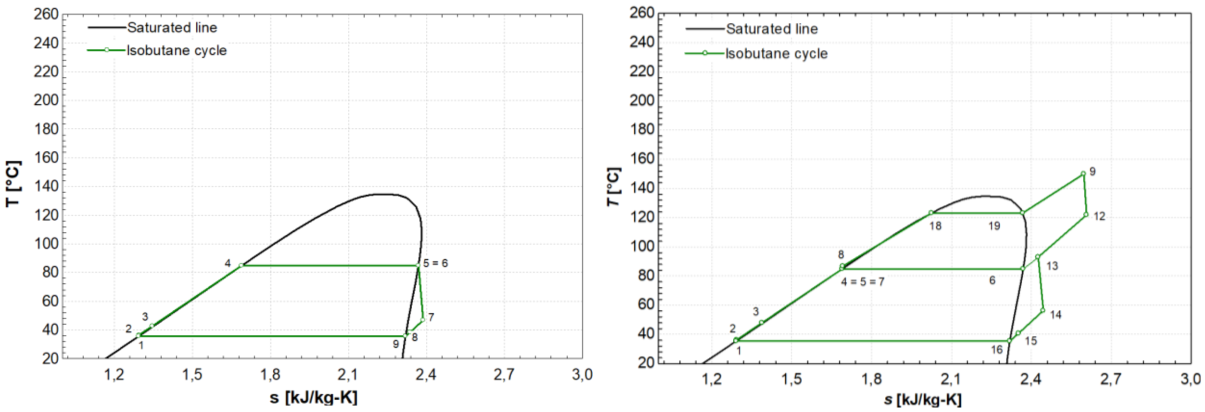


*Figure 2. T-s diagram for the thermodynamic processes of the two ORC power plants*

In Table 4, the performance indicators obtained for the evaluated case study are presented in terms of mechanical power $\dot{W}$ and thermal power $\dot{Q}$. The subscript *Cond,tot* refers to the condenser and the de-superheater.

Table 4. Performance parameters of the ORC system.

| | | | |
|---|---|---|---|
| $\eta_{ORC}$ [%] | 11.92 | $\dot{W}_{hpp}$ [MW] | 0.22 |
| $\eta_{I,Sys}$ [%] | 9.31 | $\dot{W}_{hpt}$ [MW] | 1.45 |
| $\eta_{II,Sys}$ [%] | 18.45 | $\dot{Q}_{ECO}$ [MW] | 24.01 |
| $\dot{W}_{BHP}$ [MW] | 1.99 | $\dot{Q}_{EVA}$ [MW] | 44.06 |
| $\dot{W}_{lpp}$ [MW] | 0.55 | $\dot{Q}_{Cond,tot}$ [MW] | 76.77 |
| $\dot{W}_{LPT}$ [MW] | 9.71 | $\dot{Q}_{PTCs}$ [MW] | 19.08 |

The net power obtained from the plant keeping the amount of brine extracted fixed is 8.401 MW. This enatails an increase of 3.401 MW compared to the traditional geothermal plant, which corresponds to around 68%. Specifically, 7168 kW are produced by the LP section of the system, and 1232 kW are provided by its HP section.

The values of $\eta_{ORC}$ and $\eta_{sys}$ calculated for the single geothermal plant are 10.27% and 7.03%, respectively. It is worth noticing that $\eta_{ORC}$ does not consider the BHP. The values for the hybrid geothermal-solar device are 11.92% and 9.31%, respectively. Therefore, the enhancements of the first law efficiencies in the new hybrid geothermal-solar power plant are about 16% and 32%, respectively.

## 5. Thermodynamic analysis in off-design conditions

An off-design model of the power plant was developed to assess the overall energy production over a year, given that the operating condition change with the solar irradiance and ambient temperature. The off-design model was developed considering the LMTD method for heat exchangers and implementing the characteristic curves of the turbine. Clear sky condition during daylight hours was considered for the analysis. The variations of ambient temperature and DNI were considered by imposing the variability of the flow rate of the geothermal fluid and the evaporator pressure. In Figure 3, the results of the thermodynamic analysis in off-design conditions are presented.

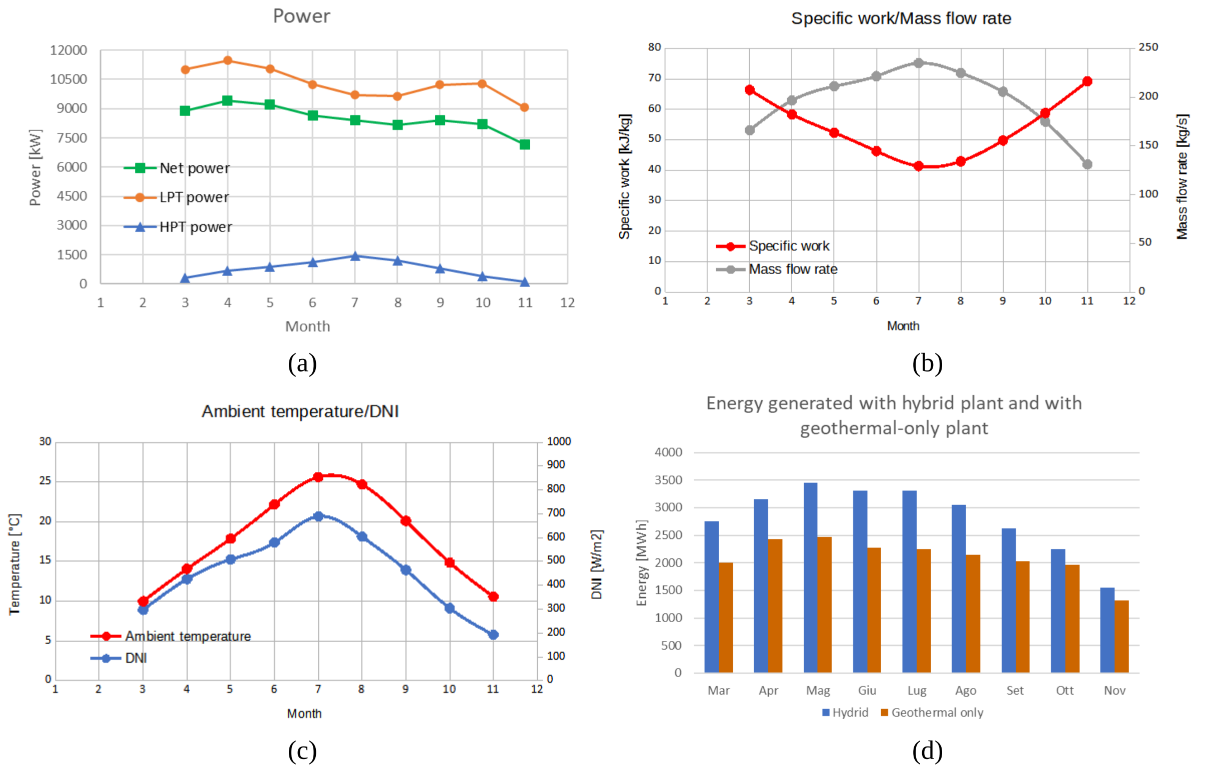


*Figure 3. (a) Monthly distribution of HPT, LPT, and a net power of the hybrid device; (b) specific work and mass flow rate of the LPT of each month; (c) ambient temperature and DNI during the year; (d) comparison of the energy generation with the traditional and hybrid systems*

The trend of the net power of the new hybrid power plant in off-design conditions is mainly determined by the low-pressure turbine as its contribution is higher than the high-pressure turbine (Figure 3a). In particular, the behavior of the LPT power depends on its specific work and mass flow rate (Figure 3b). The specific work increases as the ambient temperature decreases, lowering the pressure of the condenser. The trend of the power of the high-pressure turbine strictly follows that of the DNI throughout the year (Figure 3c). The energy transformed by the system operating with the hybrid configuration is greater than the traditional configuration during the entire year (Figure 3d). The hybridization allows increasing energy harvesting of 6555 MWh. Since a family with four people consumes around 2700 kWh per year, it is possible to provide energy to additional 2400 families.

## 6. Exergy analysis at the design point

The most impacting components of the power plant in terms of inefficiencies can be identified, as shown in Figure 4, by applying the exergy analysis.The second principle efficiency of the plant is 29.37% for the traditional geothermal system and 18.45% for the hybrid system proposed. This kind of worsening result is present in literature [28].

In fact, as noticeable in Figure 4, the new solar field is responsible for the largest exergy destruction. This destruction cannot be removed as it is inherent with the collectors energy conversion process. For this reason, a marginal second law efficiency $\eta_{II,m}$ not accounting for the exergy loss of the collectors, can be defined. The value of the marginal efficiency for the hybrid system is 41.9%, which far greater than the value for the geothermal-only power plant.

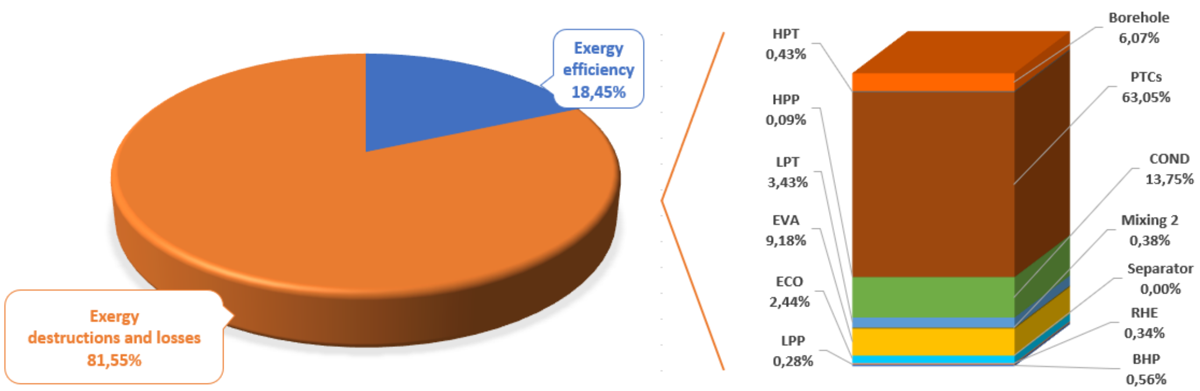


*Figure 4. Values of second law efficiency and exergy destruction and loss*

## 7. Exergo-economic and exergo-environmental analyses

The specific investment cost of the system is 6513€/kW excluding the cost of the wells. This value should be compared with the expected cost provided by IRENA [37] for a geothermal plant (between 2584€/kW and 5353€/kW) and for a concentrating solar plant (between 4060€/kW and 4800€/kW). Hence the relative cost of the proposed system is above the expected value.
The results of the exergo-economic analysis are presented in Tables 5 and Figure 5. The most expensive components of the power plant in terms of purchased equipment cost (PEC) are the solar collector field and the condenser unit due to the large surfaces needed owing to the low efficiency of the system for the moderate temperature level of the resource. Moreover, a high cost is attributable to the low-pressure turbine and the BHP. Considering also the cost of the exergy destruction ($\dot{Z}_k + \dot{C}_{D,k}$), the most impactant component is the condenser due to the very high cost and the important exergy distruction, followed by the collector field, the LP turbine, and the evaporator.

The LCOE of the new hybrid geothermal and solar power plant is 0.15$/kWh. This value is typical for solar photovoltaic systems, and it is only slightly higher compared to concentrating solar devices, as shown in *Figure 6*. The total purchased equipment cost of the system is 54.7 M€ including BHP and the cost of wells drilling is 38 M€.

*Figure 7* compares the environmental footprint of the power generated in the analyzed hybrid geothermal and solar power cycles. The construction of geothermal wells provides the highest contribution. It is followed by the low-pressure turbine, the piping, and the PTCs. The environmental impact of the isobutene as a working fluid is negligible.

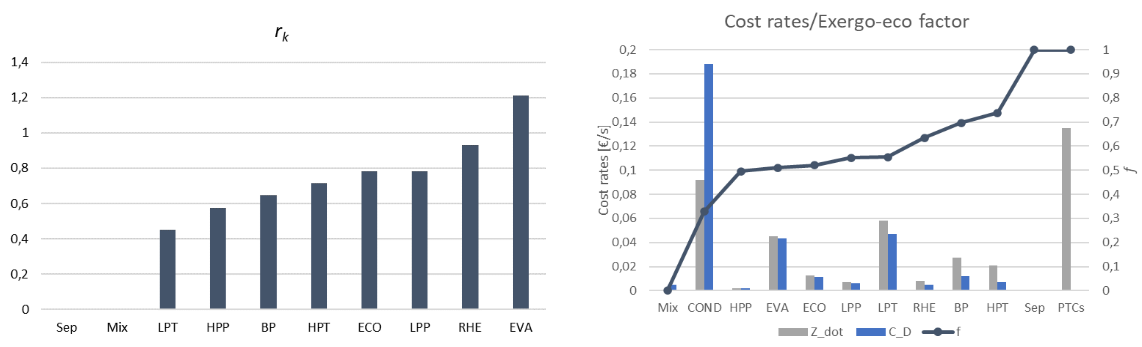


(a) (b)

*Figure 5. (a) Relative cost difference and (b) cost rates and exergo-economic factor of the main system components*

*Table 5. Outcomes of the exergo-economic analysis for the isobutane hybrid cycle*

| **Component** | **PEC (€)** | $\dot{Z}_k$ (€/s) | $\dot{C}_{D,k}$ (€/s) | $\dot{Z}_k + \dot{C}_{D,k}$ (€/s) | $c_{F,k}$ (€/kWh) | $c_{P,k}$ (€/kWh) | $r_k$ (–) | $f_k$ (–) |
|---|---|---|---|---|---|---|---|---|
| BHP | 3.380E+06 | 0.0272 | 0.01188 | 0.03910 | 0.20565 | 0.33823 | 0.64467 | 0.69612 |
| LPP | 897597 | 0.0072 | 0.00468 | 0.01281 | 0.13260 | 0.36680 | 0.78360 | 0.55156 |
| RHE | 1.009E+06 | 0.0081 | 0.01146 | 0.02391 | 0.04560 | 0.25588 | 0.92968 | 0.63474 |
| ECO | 1.545E+06 | 0.0125 | 0 | 0.00024 | 0.13207 | 0.08120 | 0.78083 | 0.52066 |
| Separator | 30155 | 0.0002 | 0.04318 | 0.08830 | 0.04560 | 0.13220 | 0.00095 | 1 |
| EVA | 5.602E+06 | 0.0451 | 0.00588 | 0.01311 | 0.20565 | 0.10095 | 1.21402 | 0.51101 |
| LPT | 7.243E+06 | 0.0583 | 0.04696 | 0.10530 | 0.13260 | 0.19269 | 0.45321 | 0.55402 |
| COND | 1.141E+07 | 0.0919 | 0.18807 | 0.27999 | 0.13260 | 0 | -1 | 0.32830 |
| HPP | 250067 | 0.0020 | 0.00205 | 0.00406 | 0.20565 | 0.32342 | 0.57262 | 0.49617 |
| PTCs | 1.566E+07 | 0.1352 | 0 | 0.13520 | 0 | 0.18845 | - | 1 |
| HPT | 2.622E+06 | 0.0211 | 0.00752 | 0.02864 | 0.17036 | 0.29225 | 0.71549 | 0.73732 |
| Mixing 2 | 0 | 0 | 0.00520 | 0.00520 | 0.13188 | 0.13260 | 0.00548 | 0 |

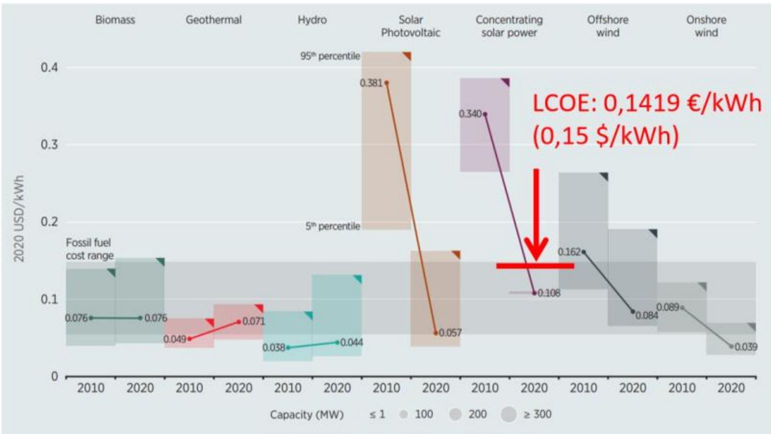


*Figure 6. Values of the LCOE of different technologies for renewable energy harnessing [37]*

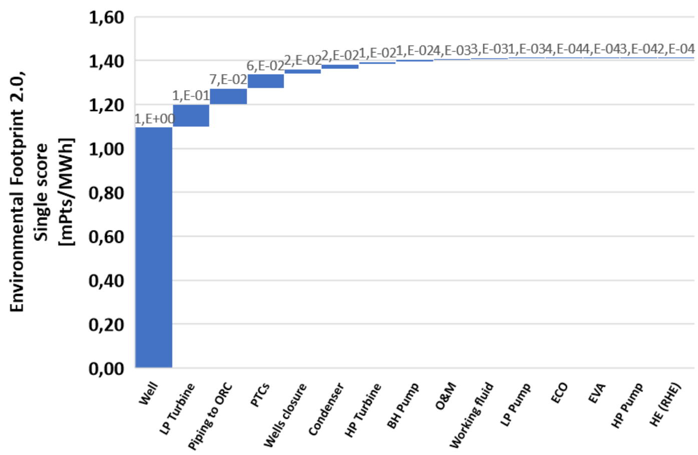


*Figure 7. Comparison of EF 2.0 single score environmental impacts of electricity produced in the hybrid geothermal and solar plant*

In Figure 8, the environmental footprint of the hybrid power cycle is compared with other renewable energy systems. Previous literature studies comparing different electricity technologies report the value of the environmental impact of electricity produced with geothermal power plants in the range between wind and photovoltaic systems for the most relevant LCA categories [29]. These studies referred to cases without NCGs sequestration. The results reported in [19] showed that electricity from binary geothermal systems has an extremely interesting overall environmental performance.

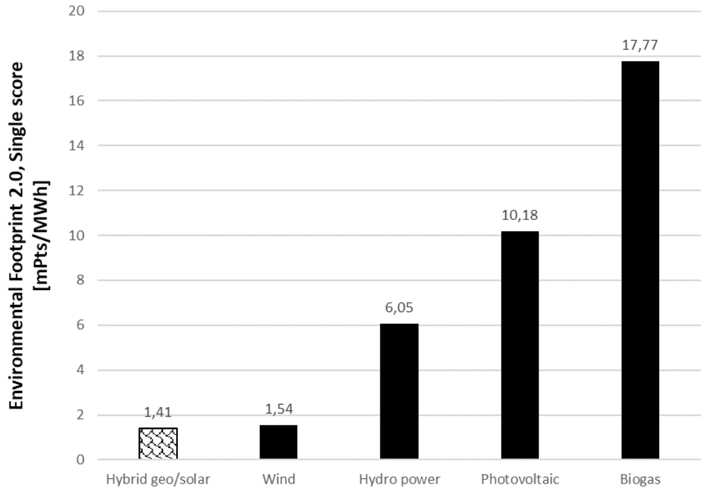


*Figure 8. Comparison of the environmental footprint 2.0 single score of the electricity produced in the hybrid geothermal and solar plant and in other renewable power systems*

*Table 6* and *Figure 9* define the results of the exergo–environmental analysis. The collector field has the highest EF score, followed by the low-pressure turbine. The PTCs have the greatest component-related environmental influence $\dot{Y}_k$. On the other hand, the higher value of total exergo-environmental impact ($\dot{Y}_k + \dot{B}_{D,k}$) is attributed to the condenser, which was also the component with the highest total environmental impact rate in the conventional geothermal plant. Moreover, the evaporator, the low-pressure turbine, and the field of collectors have relevant overall influence values. Depending on the share of $\dot{Y}_k$ or $\dot{B}_{D,k}$, performance enhancements can be recommended for components having low $\dot{Y}_k$ and high $\dot{B}_{D,k}$ as the condenser, evaporator, and low-pressure turbine. Conversely, improvements regarding the design and material economy are suggested for components with low $\dot{B}_{D,k}$ and high $\dot{Y}_k$. The component deserving the most extensive attention is the condenser owing to its greater exergy losses and relevant $\dot{B}_{D,k}$.

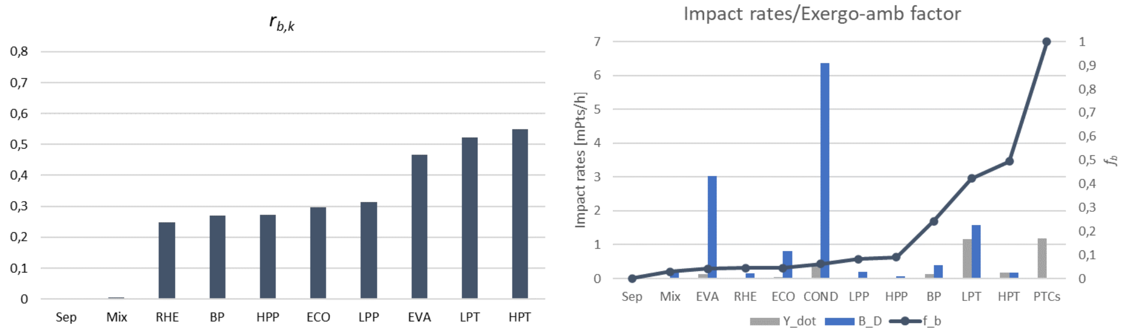


(a) (b)

*Figure 9. (a) Relative difference of specific environmental impacts; (b) Environmental impact factor (mPts/s), Exergo-environmental impact factor (mPts/s) and exergo-environmental factor*

Table 6. Exergo-environmental results for the isobutane cycle

| **Component** | **EF 2.0 Single Score (Pts)*** | $\dot{Y}_k$ **(mPts/h)** | $\dot{B}_{D,k}$ **(mPts/h)** | $\dot{B}_{D,k} + \dot{Y}_k$ **(mPts/s)** | $r_{D,k}$ **(%)** | $f_{D,k}$ **(%)** |
|---|---|---|---|---|---|---|
| BHP | 27.85 | 0.125 | 0.390 | 0.515 | 0.26933 | 0.2431 |
| LPP | 3.869 | 0.017 | 0.193 | 0.210 | 0.31253 | 0.08240 |
| RHE | 1.6199 | 0.007 | 0.158 | 0.166 | 0.24918 | 0.04379 |
| ECO | 8.341 | 0.037 | 0.804 | 0.841 | 0.29555 | 0.04439 |
| Separator | 0 | 0 | 0 | 0 | 0 | 0 |
| EVA | 29.066 | 0.130 | 3.028 | 3.158 | 0.46607 | 0.04120 |
| LPT | 259.3 | 1.161 | 1.590 | 2.750 | 0.52287 | 0.42198 |
| COND | 94.608 | 0.424 | 6.367 | 6.790 | -1 | 0.06237 |
| HPP | 1.49 | 0.007 | 0.067 | 0.074 | 0.27357 | 0.09043 |
| PTCs | 265.602 | 1.189 | 0 | 1.189 | Infinite | 1 |
| HPT | 38.5 | 0.172 | 0.176 | 0.348 | 0.54840 | 0.49551 |
| Mixing 2 | 1.182 | 0.005 | 0.176 | 0.181 | 0.00615 | 0.02918 |

## 8. Conclusions

The present research aims at analyzing the economic and environmental characteristics of a hybrid power plant consisting of a closed binary bottomer geothermal cycle and a topper concentrating solar cycle. The obtained results are compared with those of a traditional geothermal configuration.

Once the solar direct normal irradiance data for the typical monthly day was defined, a complete thermodynamic analysis in design conditions was conducted. The net power obtained from the plant is 8.401 MW. The integration of the solar system increases net power transformation by about 68% compared to the traditional geothermal plant. This results in an efficiency enhancement from 7.03% to 9.31%.

An initial off-design analysis was performed to estimate the behavior of the net power by varying the ambient temperature and the DNI. The trend of the net power of the new hybrid power plant follows that of the low-pressure turbine as its contribution is higher regarding the high-pressure turbine. In particular, the behavior of the low-pressure turbine power is similar to that of its specific work and mass flow rate. The specific work improves as the ambient temperature reduces. When the ambient pressure decreases, the temperature and pressure at the condenser decrease. This extends the expansion and, thus, enhances the specific work. The hybridization increases energy harnessing by 6555 MWh.

The exergy analysis showed a depletion in the second principle efficiency of the new plant compared to the conventional one. A value of 0.1845 was obtained for the new plant compared to the value of 0.2937 of the original system. Lowering the exergy efficiency is attributed to the high losses and destructions of exergy due to the solar collectors. It is possible to define a marginal exergy efficiency not considering the exergy losses of the collectors, that is equal to 0.419.

The specific investment cost of the new hybrid plant was found to be 6513 €/kW. The cost analysis showed that the solar field has the highest cost. The exergo-economic analysis showed that PTCs also have the highest instantaneous capital cost $Z$. Due to its high heat exchange surface, the condenser is a very expensive component, second only to the solar field. The LCOE value is 14.19 c€/kWh. It is in the range of the solar photovoltaic and slightly higher than that of concentrating solar power.

Concerning the exergo-environmental analysis, the component with the highest environmental impact rate $\dot{Y}$ is the solar array. The condenser has the highest total environmental impact rate.

## References

[1] Kagel, A., Bates, D. and Gawell, K. (2005). A guide to geothermal energy and the environment. Geothermal Energy Association, Washington, DC (USA). https://doi.org/10.2172/897425

[2] Rice, K. M., Walker, E. M., Wu, M., Gillette, C. and Blough, E. R. (2014). Environmental mercury and its toxic effects. In *Journal of Preventive Medicine and Public Health*. https://doi.org/10.3961/jpmph.2014.47.2.74

[3] Baldacci, A., Mannari, M. and Sansone, F. (2005). Greening of Geothermal Power: An Innovative Technology for Abatement of Hydrogen Sulphide and Mercury Emission. World Geothermal Congress 2005, April.

[4] Bruscoli, L., Fiaschi, D., Manfrida, G. and Tempesti, D. (2015). Improving the environmental sustainability of flash geothermal power plants-A case study. *Sustainability*, *7*(11), 15262–15283. https://doi.org/10.3390/su71115262

[5] Eberle, A., Heath, G., Nicholson, S., Carpenter, A., Eberle, A., Heath, G., Nicholson, S. and Carpenter, A. (2017). *Systematic Review of Life Cycle Greenhouse Gas Emissions from Geothermal Electricity*. *September*.

[6] Bates, M. N., Crane, J., Balmes, J. R. and Garrett, N. (2015). Investigation of Hydrogen Sulfide Exposure and Lung Function, Asthma and Chronic Obstructive Pulmonary Disease in a Geothermal Area of New Zealand. 1–16. https://doi.org/10.1371/journal.pone.0122062

[7] Hartmann, J. and Rydgren, B. (2018). Geothermal Sustainability Assessment Protocol Hellisheidi Geothermal Project GSAP.

[8] Peralta, O., Castro, T., Durón, M., Salcido, A., Celada-murillo, A., Navarro-gonzález, R., Márquez, C., García, J., De, J., Torres, R., Villegas-martínez, R., Carreón-sierra, S., Imaz, M., Martínez-arroyo, A., Saavedra, I., De, M., Espinosa, L. and Torresjaramillo, A. (2013). Geothermics $H_2S$ emissions from Cerro Prieto geothermal power plant , Mexico , and air pollutants measurements in the area. Geothermics, 46, 55–65. https://doi.org/10.1016/j.geothermics.2012.12.001

[9] Duan, Z. and Sun, R. (2003). An improved model calculating CO 2 solubility in pure water and aqueous NaCl solutions from 273 to 533 K and from 0 to 2000 bar. *Chemical Geology*. https://doi.org/10.1016/S0009-2541(02)00263-2

[10] O’Sullivan, M. J., Bodvarsson, G. S., Pruess, K. and Blakeley, M. R. (1985). Fluid and Heat Flow In Gas-Rich Geothermal Reservoirs. *Society of Petroleum Engineers Journal*, *25*(2), 215–226. https://doi.org/10.2118/12102-PA

[11] Pruess, K., Oldenburg, C. M. and Moridis, G. J. (1999). TOUGH2 User’s Guide Version 2.

[12] Parkhurst, D. L. and Appelo, C. A. J. (1999). USER’S GUIDE TO PHREEQC (VERSION 2)—A COMPUTER PROGRAM FOR SPECIATION, BATCH-REACTION, ONE-DIMENSIONAL TRANSPORT, AND INVERSE GEOCHEMICAL CALCULATIONS (Issue Version 2).

[13] DGS-UNMIG, M. dello sviluppo economico. (2018b). *Pozzi geotermici*. http://unmig.mise.gov.it/unmig/geotermia/pozzi/pozzi.asp (accessed 12.25.18).

[14] DGS-UNMIG, M. dello sviluppo economico. (2018a). *Inventario delle risorse geotermiche nazionali*. http://unmig.sviluppoeconomico.gov.it/unmig/geotermia/inventario/inventario.asp (accessed 12.25.18).

[15] Buonasorte, G., Cataldi, R., Ceccarelli, A., Costantini, A., D’Offizi, S. and Lazzarotto, A. (1988). Ricerca ed esplorazione nell’area geotermica di Torre Alfina (Lazio-Umbria). *Boll.Soc.Geol.It.*, 265–337.

[16] Buonasorte, G., Pandeli, E. and Fiordelisi, A. (1991). The Alfina 15 well: deep geological data from Northern Latium (Torre Alfina geothermal area). *Boll.Soc.Geol.It.*, 823–831.

[17] Regione Umbria and Università di Perugia. (2013). *Studio delle potenzialità geotermiche del territorio regionale umbro Report finale*.

[18] DGS-UNMIG, M. dello sviluppo economico. (2019). *Ricerca di risorse geotermiche finalizzata alla sperimentazione di Impianti Pilota*. https://unmig.mise.gov.it/index.php/it/dati/risorse-

geotermiche/ricerca-di-risorse-geotermiche-finalizzata-allasperimentazione-di-impianti-pilota (accessed 5.9.19).
[19] Fiaschi, D., Leveni, M., Manfrida, G., Mendecka, B., Talluri. L., Zuffi, C. (2021). Geothermal power plants with improved environmental performance: assessment of the potential for an Italian site.
[20] Bejan, A., Tsatsaronis, G. and Moran, M. J. (1996). *Thermal Design and Optimization*. John Wiley and Sons. https://doi.org/10.1016/S0140-7007(97)87632-3
[21] Klein, S. and Nellis, G. (2012). *Mastering EES, f-Chart software*.
[22] Lazzaretto, A. and Tsatsaronis, G. (2006). SPECO: A systematic and general methodology for calculating efficiencies and costs in thermal systems. *Energy*. https://doi.org/10.1016/j.energy.2005.03.011
[23] Mwawasi, H. M. (2014). *Feasibility study of using a downhole pumping system in Menengai well MW -17 for geothermal utilization.*
[24] Turton, R. (2013). Analysis, Synthesis, and Design of Chemical Processes Fourth Edition. In *Journal of Chemical Information and Modeling*.
[25] Dumas, P., Antics, M. and Ungemach, P. (2013). *Report on geothermal drilling*. http://www.geoelec.eu/wpcontent/uploads/2011/09/D-3.3-GEOELEC-report-on-drilling.pdf (accessed on 12/07/2019).
[26] Fiaschi, D., Manfrida, G., Rogai, E. and Talluri, L. (2017). Exergoeconomic analysis and comparison between ORC and Kalina cycles to exploit low and medium-high temperature heat from two different geothermal sites. *Energy Conversion and Management*, *154*(November), 503–516. https://doi.org/10.1016/j.enconman.2017.11.034
[27] Cortes Felipé, Ibarra Mercedes, Moser Francisco et al. (2018), Techno-economical evaluation of parabolic trough collectors systems for steam processes in the Chilean industry
[28] Bonforte, Bucjgeister, Manfrida, Petela (2017); Exergoeconomic and Exergoenvironmental analysis of an integrated solar gas turbine/combined cycle power plant.
[29] Asdrubali, F., Baldinelli, G., D'Alessandro, F. and Scrucca, F. (2015). Life cycle assessment of electricity production from renewable energies: Review and results harmonization. *Renewable and Sustainable Energy Reviews*, *42*, 1113–1122. https://doi.org/10.1016/J.RSER.2014.10.082
[30] Italian Ministry of the Environment and Protection of Land and Sea. (2018). *Geothermal pilot plant named "TorreAlfina", Acquapendente (VT)* - *VAS* - *VIA* - *AIA*.
[31] Fiaschi, D., Manfrida, G., Ungar, P., Talluri, L. (2021). Development of an exergo-economic and exergo-environmental tool for power plant assessment: evaluation of a geothermal case study. ECOS 2021 Program Organizers, 24-35, https://doi.org/10.52202/062738-0003
[32] Huld, T., Müller, R. and Gambardella, A., 2012. "A new solar radiation database for estimating PV performance in Europe and Africa". Solar Energy, 86, 1803-1815.
[33] Odeh S. D. and Abu-Mulaweh H. I., "Design and development of an educational solar tracking parabolic trough collector system," vol. 15, no. 1, 2013.
[34] Kong Li, Zhang Yunpeng, Zhijian Lin, Qiu Zhongzhu*, Li Chunying, Le Ping; "Optimal design of the solar tracking system of parabolic trough concentration collectors"; 2020; *International Journal of Low-Carbon Technologies*, Volume 15, Issue 4, November 2020, Pages 613–619, https://doi.org/10.1093/ijlct/ctaa065
[35] Duffie John A., Beckman William A., Blair Nathan; "Solar engineering of thermal processes, photovoltaics and wind", fifth edition, Wiley, 2020
[36] Manfrida Giampaolo, Gerard Vincent (2008); "Maximum exergy control of a Solar thermal plant equipped with direct stream collectors"; International journal of thermodynamics; volume ii, issue 3; 143-149
[37] IRENA (2021), Renewable Power Generation Costs in 2020, International Renewable Energy Agency, Abu Dhabi